Breast Cancer Research and Treatment (2019) 177:629–639
https://doi.org/10.1007/s10549-019-05342-5

PRECLINICAL STUDY

Non-contrast MRI for breast screening: preliminary study on detectability of benign and malignant lesions in women with dense breasts

Yangyang Bu[1,2] · Jun Xia[3] · Bobby Joseph[4] · Xianjing Zhao[1,2] · Maosheng Xu[1,2] · Yingxing Yu[1,2] · Shouliang Qi[5] · Kamran A. Shah[4] · Shiwei Wang[1,2] · Jiani Hu[4]

Received: 16 April 2019 / Accepted: 29 June 2019 / Published online: 19 July 2019

Abstract

Purpose The importance of breast cancer screening has long been known. Unfortunately, there is no imaging modality for screening women with dense breasts that is both sensitive and without concerns regarding potential side effects. The purpose of this study is to explore the possibility of combined diffusion-weighted imaging and turbo inversion recovery magnitude MRI (DWI + TIRM) to overcome the difficulty of detection sensitivity and safety.

Methods One hundred and seventy-six breast lesions from 166 women with dense breasts were retrospectively evaluated. The lesion visibility, area under the curve (AUC), sensitivity and specificity of cancer detection by MG, DWI + TIRM, and clinical MRI were evaluated and compared. MG plus clinical MRI served as the gold standard for lesion detection and pathology served as the gold standard for cancer detection.

Results Lesion visibility of DWI + TIRM (96.6%) was significantly superior to MG (67.6%) in women with dense breasts ($p < 0.001$). There was no significant difference compared with clinical MRI. DWI + TIRM showed higher accuracy (AUC = 0.935) and sensitivity (93.68%) for breast cancer detection than MG (AUC = 0.783, sensitivity = 46.32%), but was comparable to clinical MRI (AUC = 0.944, sensitivity = 93.68%). The specificity of DWI + TIRM (83.95%) was lower than MG (98.77%), but higher than clinical MRI (77.78%).

Conclusions DWI combined with TIRM could be a safe, sensitive, and practical alternative for screening women with dense breasts.

Keywords Dense breasts · Non-contrast MRI · Diffusion-weighted imaging · Mammography · Breast cancer screening

Abbreviations

ADC	Apparent diffusion coefficient
AUC	Area under the curve
BI-RADS	Breast imaging reporting and data system
CC	Craniocaudal
DWI	Diffusion-weighted imaging
DWI + TIRM	Diffusion-weighted and turbo inversion recovery magnitude MRI
MG	Mammography
MLO	Mediolateral oblique
MRI	Magnetic resonance imaging
PACS	Picture archiving and communications system
ROC	Receiver operating characteristic
ROI	Region of interest
STIR	Short time inversion recovery
TIRM	Turbo inversion recovery magnitude

Introduction

Approximately 43 to 52% of women in the U.S. have dense breasts [1, 2]. Women with dense breasts have a 1.5- to 6-fold increased risk of developing breast cancer compared to their fatty density counterparts [3–5]. The three most common breast cancer screening modalities are mammography (MG), ultrasound, and magnetic resonance imaging (MRI). Unfortunately, the imaging techniques to screen

Yangyang Bu and Jun Xia contributed equally to this study.

✉ Shiwei Wang
wsw1204@zcmu.edu.cn; 2474721554@qq.com

✉ Jiani Hu
jhu@med.wayne.edu

Extended author information available on the last page of the article

women with dense breasts that are sensitive have concerns regarding their safety. As approximately half the population of women undergoing screening have dense breasts, there is a pressing need to find a sensitive, safe, and fast imaging technique for this population.

MG, the most widely used technique to screen women for breast cancer, has markedly increased the detection rate of small tumors (invasive tumors measuring < 2 cm or in situ carcinomas) [6]. As dense breasts tend to mask more masses compared to fatty breasts, the sensitivity of MG can be as low as 30–45% in these women [7, 8]. Because of the high rate of missed lesions in dense breasts, many states have enacted laws requiring women to be notified if their screening mammograms reveal dense breasts.

Ultrasound is a noninvasive imaging modality that uses the reflection of sound waves from a transducer to create images. Ultrasound is frequently used as an adjunct to MG in elevated-risk groups such as women with dense breasts [9, 10]. However, there is controversy regarding the use of ultrasound as a primary screening tool due to several drawbacks including sensitivity, specificity, scan time, and operator dependence [11, 12].

MRI uses a magnetic field to capture signals from water protons in the body and can provide anatomic as well as functional information. Contrast-enhanced MRI is included in the standard protocol for screening women with a high risk of breast cancer, such as those with a lifetime risk > 20–25% [13]. According to a systematic review, the use of MRI for high risk women improved the sensitivity of lesion detection by MG from 32 to 84% [14]. MRI has been considered the most sensitive and safe screening modality due of its non-invasive nature, excellent contrast for soft tissues, and capability of providing information on anatomy and function. Although no conclusion has been reached on the safety of repeated gadolinium exposure from MRI contrast agents, the recent discovery of deposition and accumulation of gadolinium-based contrast agents in the brain raises concerns regarding the safety of contrast-enhanced MRI as a tool for life long breast cancer screening [15–18]. Moreover, the use of MRI contrast agent adds expense to the already costly MRI examination.

Diffusion-weighted imaging (DWI) is a functional MRI technique that reflects the random movement of free water molecules known as Brownian motion. Hindrance in the diffusion of water molecules is proportional to the degree of cellularity of the tissue. Restricted diffusion occurs in tissues with higher cellular density, like most cancers, and is depicted as hyperintense on DWI [19, 20]. ADC values calculated from DWI further improve accuracy in differentiating between benign and malignant breast lesions [21–23]. Several studies have investigated DWI as an adjunct screening tool to MG and demonstrated its usefulness in detecting breast cancer in elevated-risk women with dense breasts [24, 25]. Turbo inversion recovery magnitude (TIRM) is one of the commonly used MRI pulse sequences of breast MRI. It is a type of inversion recovery MRI sequence with the advantages of a short image acquisition time. Additionally, compared with conventional T1-weighted and T2-weighted images, TIRM is more suitable for fat suppression of breast tissue. [26]. As such, TIRM has been widely used in delineation of tumor and lymphatic spread [27]. The objective of this study is to explore the potential of a single MRI exam with only two sequences: DWI and TIRM. To accomplish this goal, we evaluated and compared lesion visibility as well as the area under the curve (AUC), sensitivity and specificity of cancer detection by MG, DWI + TIRM, and clinical MRI. MG plus clinical MRI were used as the gold standard for lesion detection while pathology served as the gold standard for cancer detection.

Materials and methods

Patients

This retrospective study was approved by the institutional review board and the informed consent requirement was waived. Between January 2014 and December 2016, a total of 5292 inpatients that underwent breast biopsy or surgery were identified through a review of the medical records. Within this group, we selected patients who met the following criteria: (1) underwent both MG and breast MRI at our institution within 1 month prior to their first biopsy or surgery; (2) did not receive chemo-radiotherapy before surgery; (3) had breast lesions detected on MG and/or MRI. We identified 214 patients who met these criteria. We excluded patients in whom the period between MG and breast MRI examinations was more than 2 weeks to maintain the consistency between the two imaging results and the pathology. (n = 25). We also excluded patients whose breasts were not classified as heterogeneously dense or extremely dense according to Breast Imaging Reporting and Data System (BI-RADS) [28] (n = 23). A total of 166 patients with 176 breast lesions were included in this study (Fig. 1).

Mammography

All the MG images were acquired with the Mammomat Inspiration® mammograph (Siemens, Erlangen, Germany). Patients underwent MG imaging of both breasts in the mediolateral oblique (MLO) and craniocaudal (CC) position with automatic exposure.

MR imaging protocol

MRI examinations were performed in a 3.0 T MR system (Magnetom Verio, Siemens, Erlangen, Germany) in combination with a dedicated 16-channel breast coil. Images of both breasts were acquired with the patient in prone position. The imaging protocol consisted of (1) TIRM sequence (TR/TE/TI = 4000/70/230 ms, FOV = 360 × 360 mm, matrix 448 × 448, slice thickness 4 mm, NEX 2, resulting in a voxel size of 1.1 × 0.8 × 4.0 mm^3, sequence duration of 2 min 48 s); (2) DWI, obtained using echo planar imaging (TR/TE = 8400/84 ms, FOV = 360 × 360 mm, matrix 220 × 220, slice thickness 4 mm, NEX 3, b0 = 50 s/mm^2, b1 = 400 s/mm^2, b2 = 800 s/mm^2, resulting in a voxel size of 1.8 × 1.6 × 4.0 mm^3, sequence duration of 2 min 56 s). Apparent diffusion coefficient (ADC) values were calculated automatically by the MR imaging system software from the DWI images. (3) The dynamic contrast-enhanced MR imaging sequences were performed by using the following parameters: TR/TE = 4.51/1.61 ms, flip angle = 10°, FOV = 340 × 340 mm, matrix 448 × 448, slice thickness 1 mm, NEX 1. Dynamic contrast-enhanced axial MR imaging was performed with one pre-contrast and five post-contrast dynamic series. Contrast-enhanced images were acquired at 5, 65, 125, 185, and 245 s after contrast injection. Gadobenate dimeglumine (BeiLu Pharmaceutical, Beijing, China) was intravenously injected at a dose of 0.1 mmol/kg of body weight and flow rate of 2.0 ml/s followed by 10 ml of saline solution.

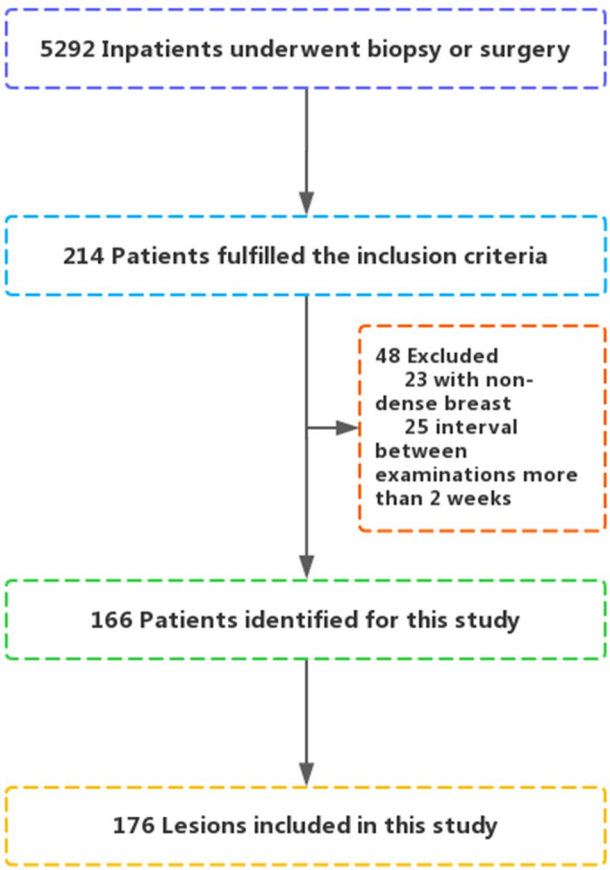

Fig. 1 Flow diagram of enrolled patients. Of the 5292 inpatients who underwent biopsy or surgery, only 214 met the inclusion criteria. After excluding 48 people who were either not classified as having dense breasts or had an interval of more than 2 weeks between MG and MRI, 166 women and 176 lesions were finalized for this study

Image interpretation

All examinations were evaluated independently by two radiologists who have 10 and 27 years of breast MRI experience, respectively. Radiologists were blind to clinical, laboratory, and other imaging findings. All cases were electronically placed in the picture archiving and communications system (PACS) and reviewed in a random order, differently sorted for MG and MRI including DWI and DWI + TIRM. MR readings were performed initially with TIRM and a combination of DWI and ADC maps (DWI + TIRM) then finally including the rest of the sequences (clinical MRI). For each patient and for each image modality (MG, DWI + TIRM, and clinical MRI), the interpreters scored for the presence or absence of breast lesions using an ordinal scale with 1, definitely or almost definitely absent; 2, probably absent; 3, possibly present; 4, most likely present; and 5, definitely or almost definitely present. Scores of 3, 4, and 5 were regarded as positive findings for lesion visibility [24]. The two interpreters also recorded the location of every lesion. For patients with two or more lesions, each lesion was rated by the interpreting radiologist. The interpreters scored for the level of suspicion for malignancy using the same ordinal scale with 1, definitely or almost definitely absent; 2, probably absent; 3, possibly present; 4, most likely present; and 5, definitely or almost definitely present. Scores of 3, 4, and 5 were regarded as positive findings for tumor visibility [24]. The radiologists distinguished lesion versus tumor by using the stated criteria in combination with ADC maps as well as the anatomic and morphologic characteristics on imaging. MG plus clinical MRI was used as the gold standard for lesion detection. Pathology was used as the gold standard for diagnosis of the lesion. Inter-observer discrepancies were resolved through consensus. A representative case is shown in Figs. 2, 3, and 4.

ADC measurements

In order to maintain consistency, one radiologist performed the ROI measurements using GE Healthcare

Centricity Radiology RA600 V8.0 software after all the lesions were given a score. A region of interest (ROI) was drawn in the highest intensity part of the lesion in the slice of maximum area of the lesion on $b = 800$ s/mm^2 DWI images and subsequently copied to the ADC map.

Statistical analysis

Statistical analyses were performed using SPSS Version 24.0 (IBM, Armonk, NY) and MedCalc Version 15.2.2 (MedCalc, Inc., Mariakerke, Belgium).

Cochran's Q test was used to investigate the difference in lesion visibility between MG, DWI + TIRM, and clinical MRI. Analyses of subgroups comparing MG, DWI + TIRM, and clinical MRI lesion visibility were also evaluated with the Cochran's Q test, including patient age (< 45 years old, ≥ 45 years old), menopausal status (premenopausal, postmenopausal), lesion size (< 8 mm, ≥ 8 mm), and pathology (benign, malignant). Scores of 3, 4, and 5 were regarded as positive findings. The significance level of related samples of Cochran's Q test and pairwise comparisons were 0.05 and 0.0167 (0.05/3), respectively.

For analysis of single diagnostic method, including (1) MG, (2) DWI + TIRM, and (3) clinical MRI, receiver operating characteristic (ROC) curves were generated and the areas under the curve (AUCs) calculated and compared using the method of DeLong et al. [29]. ADC values to differentiate between benign and malignant lesions were also examined using ROC curves. Statistical significance was attained when $p \leq 0.05$.

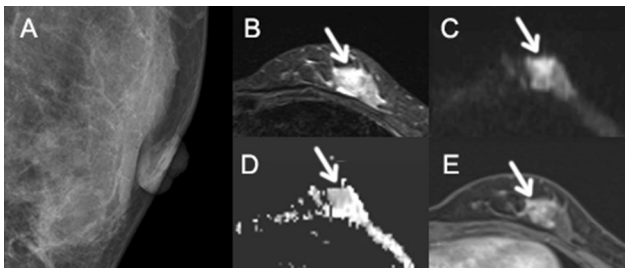

Fig. 2 A 35-year-old woman with dense breasts, with pathologically proven invasive carcinoma of no special type in the left breast. The lesion visibility scores of MG, DWI + TIRM, and clinical MRI of this patient were 2, 4, and 5, respectively. The breast cancer detection scores of MG, DWI + TIRM, and clinical MRI of this patient were 2, 3, and 4, respectively. **a** MG showed no abnormal findings. **b** TIRM and **c** DWI ($b = 0.8 \times 10^{-3}$ s/mm^2) demonstrated high signal intensity in the left breast. **d** The ADC value of this lesion was 0.85×10^{-3} mm^2/s. **e** Contrast-enhanced MRI showed lesion enhancement

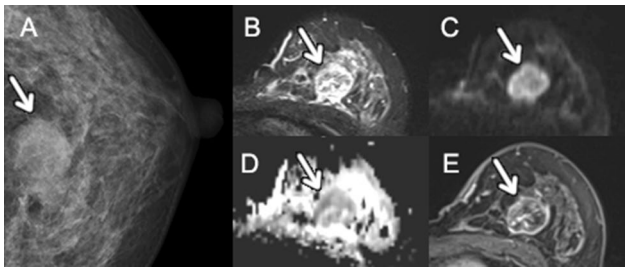

Fig. 3 A 44-year-old woman with dense breasts, with pathologically proven invasive carcinoma of no special type in the left breast. The lesion visibility scores of MG, DWI + TIRM, and clinical MRI of this patient were 4, 5, and 5, respectively. The breast cancer detection scores of MG, DWI + TIRM, and clinical MRI of this patient were 3, 4, and 5, respectively. **a** MG showed a high-density lesion with a partially obscured margin. **b** TIRM and **c** DWI ($b = 0.8 \times 10^{-3}$ s/mm^2) demonstrated a heterogeneous high-signal-intensity lesion in the left breast. **d** The ADC value of this lesion was 1.03×10^{-3} mm^2/s. **e** Contrast-enhanced MRI showed lesion heterogeneous enhancement

Results

Patient demographic and lesion characteristics

As seen in Table 1, a total of 176 lesions in 166 women aged 22–80 years (mean age, 47.0 ± 10.9 years) were assessed in this study. Among the 166 patients, 71.1% (118) were

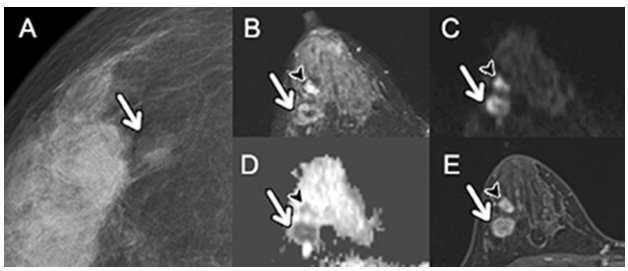

Fig. 4 A 38-year-old woman with dense breasts, with pathologically proven invasive carcinoma of no special type and mucinous carcinoma in the right breast. The lesion visibility scores of MG, DWI + TIRM, and clinical MRI of the lesion (arrow) were 4, 5, and 5, respectively. The breast cancer detection scores of MG, DWI + TIRM, and clinical MRI of the lesion (arrow) were 3, 4, and 5, respectively. The lesion visibility scores of MG, DWI + TIRM, and clinical MRI of the lesion (arrow head) were 2, 5, and 5, respectively. The breast cancer detection scores of MG, DWI + TIRM, and clinical MRI of the lesion (arrow head) were 2, 4, and 5, respectively. **a** MG showed a high-density lesion with a circumscribed margin. **b** TIRM and **c** DWI ($b = 0.8 \times 10^{-3}$ s/mm^2) demonstrated a heterogeneous high-signal-intensity lesion (arrow) and a homogeneous high-signal-intensity lesion (arrow head) in the right breast. **d** ADC values of these two lesions were 0.78×10^{-3} mm^2/s (arrow) and 0.83×10^{-3} mm^2/s (arrow head). **e** Contrast-enhanced MRI showed both lesion heterogeneous enhancement

premenopausal and 28.9% (48) were postmenopausal. Family history of breast cancer was noted in 3 patients in the study.

The lesions were determined to be benign in 81/176 (46.0%) and malignant in 95/176 (54.0%). The histopathological diagnosis included invasive carcinoma of no special type ($n=87$), fibroadenoma ($n=43$), intraductal papilloma ($n=13$), lobular hyperplasia ($n=16$), granulomatous mastitis ($n=6$), ductal carcinoma in situ ($n=5$), mucinous carcinoma ($n=2$), sclerosing adenosis ($n=2$), spindle cell carcinoma ($n=1$), as well as adenomyoepithelioma ($n=1$). Lesion sizes, as defined by the longest dimension on MRI, ranged from 3.7 to 101.6 mm (median, 18.3 (11.8, 26.6) mm).

Lesion visibility

The Cochran's Q of lesion visibility demonstrated a significant difference in lesion visibility between MG, DWI + TIRM, and clinical MRI ($p<0.001$). Only 119 (67.6%) lesions were visible on MG, while 170 (96.6%) were visible on DWI + TIRM. All lesions were detected on clinical MRI (Fig. 5).

Analysis of subsets (Table 2) found that the lesion visibility of DWI + TIRM and clinical MRI were significantly superior to MG for patient age, menopausal status, size ≥ 8 mm, and pathology. No significant differences regarding visibility were found between DWI + TIRM and clinical MRI. Clinical MRI was superior in detecting size < 8 mm compared to MG. DWI + TIRM was also superior than MG in detecting lesions < 8 mm ($p=0.001$), without reaching statistical significance ($p=0.065$).

Table 1 Summary of patient demographics and lesion characteristics

Observations	Value*
Patient demographic characteristics ($n=166$)	
Age (years)	47.0 ± 10.9#
Menopausal status	
Premenopausal	118
Postmenopausal	48
Family history of breast cancer	
With family history of breast cancer	3
Without family history of breast cancer	163
Mass characteristics ($n=176$)	
Size (mm)	22.1 ± 15.2#
Pathology	
Invasive carcinoma of no special type	87
Fibro adenoma	43
Lobular hyperplasia	16
Intraductal papilloma	13
Granulomatous mastitis	6
Ductal carcinoma in situ	5
Mucinous carcinoma	2
Sclerosing adenosis	2
Spindle cell carcinoma	1
Adenomyoepithelioma	1

*Number (except for those marked with #)

Mean ± SD

Lesion invisibility

Of 176 lesions, 6 were invisible on DWI + TIRM. Pathology types of these missed lesions are shown in Table 3 and include fibroadenoma ($n=2$), intraductal papilloma ($n=1$), and lobular hyperplasia ($n=3$).

In contrast, 57 lesions were invisible on MG. Of these, 47 were determined to be benign and 10 were found to be malignant. The pathologies of these missed lesions are also depicted in Table 3 and include invasive carcinoma of no special type ($n=8$), mucinous carcinoma ($n=2$), fibroadenoma ($n=23$), intraductal papilloma ($n=10$), lobular hyperplasia ($n=9$), granulomatous mastitis ($n=2$), sclerosing adenosis ($n=2$), and adenomyoepithelioma ($n=1$).

Only 4 of the invisible lesions on DWI + TIRM were < 8 mm compared to 11 on MG (Fig. 6). Among these missed lesions < 8 mm, 1 malignant lesion was missed on MG, while no malignant lesions were missed on DWI + TIRM. Similarly, MG missed 10 benign lesions < 8 mm while only 4 were missed on DWI + TIRM.

Two invisible lesions on DWI + TIRM measured 8 mm, while 46 missed lesions on MG were larger than 8 mm (Fig. 6). In total, 9 malignant lesions larger than 8 mm were missed on MG, while no malignant lesions of this size were missed on DWI + TIRM. As for benign masses greater than 8 mm, 37 were missed on MG compared to the 2 missed on DWI + TIRM. Thus, while MG missed malignant lesions of all sizes, DWI + TIRM only missed benign lesions.

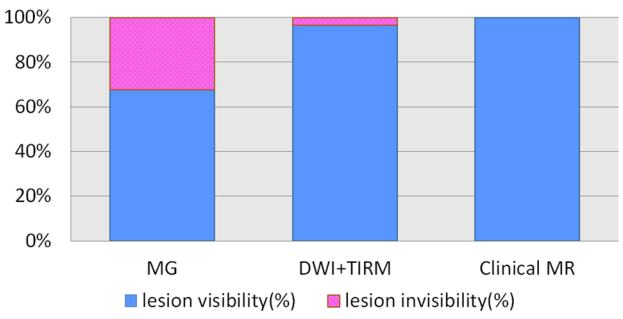

Fig. 5 Lesion visibility and invisibility of MG, DWI + TIRM, and clinical MRI

Table 2 Comparison of lesion visibility by MG, DWI + TIRM, and clinical MRI

	MG		DWI + TIRM		Clinical MRI		*p* Values		
	−	+	−	+	−	+	MG and DWI + TIRM	MG and clinical MRI	DWI + TIRM and clinical MRI
All lesion	57	119	6	170	0	176	< 0.001	< 0.001	0.339
Patient age									
Age < 45	28	46	3	71	0	74	< 0.001	< 0.001	0.487
Age ≥ 45	29	73	3	99	0	102	< 0.001	< 0.001	0.509
Menopausal status									
Premenopausal	47	80	5	122	0	127	< 0.001	< 0.001	0.377
Postmenopausal	10	39	1	48	0	49	0.001	< 0.001	0.712
Lesion size									
< 8 mm	11	1	4	8	0	12	0.065	0.001	0.140
≥ 8 mm	46	118	2	162	0	164	< 0.001	< 0.001	0.721
Pathology									
Benign	47	34	6	75	0	81	< 0.001	< 0.001	0.294
Malignant	10	85	0	95	0	95	< 0.001	< 0.001	1

Table 3 Pathology of the invisible lesions on DWI + TIRM and MG

	IC-NST	MC	FA	IP	LH	GM	SA	AME
DWI + TIRM	0	0	2	1	3	0	0	0
MG	8	2	23	10	9	2	2	1

More lesions were missed on MG compared to DWI + TIRM. Fibroadenoma, intraductal papilloma, and lobular hyperplasia were missed on DWI + TIRM while all pathologies were missed on MG

AME adenomyoepithelioma, *FA* fibroadenoma, *GM* granulomatous mastitis, *IC-NST* invasive carcinoma of no special type, *IP* intraductal papilloma, *LH* lobular hyperplasia, *MC* mucinous carcinoma, *SA* sclerosing adenosis

ROC curves

Figure 7 and Table 4 present the ROC curve figures and analysis of all three imaging modalities (MG, DWI + TIRM, and clinical MRI).

The diagnostic accuracies of MG, DWI + TIRM, and clinical MRI, measured by AUC, were 0.783, 0.935, and 0.944, respectively. The sensitivities of these modalities were 46.32%, 93.68%, and 93.68%, respectively. The specificities of these modalities were 98.77%, 83.95%, 77.78%, respectively. The AUC of MG was significantly inferior to DWI + TIRM and clinical MRI ($p < 0.001$). No significant differences in AUC were found between DWI + TIRM and clinical MRI.

ADC values had high accuracy in differentiating benign from malignant tumors (AUC = 0.899; 95% CI 0.845–0.939; sensitivity = 77.89%, specificity = 93.83%, cutoff = 0.99×10^{-3} mm^2/s) (Fig. 8).

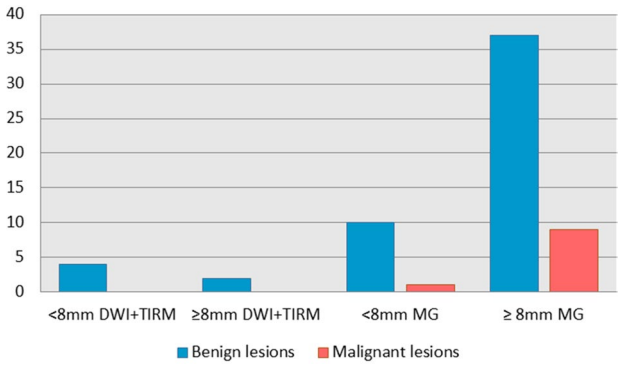

Fig. 6 Numbers of the invisible lesions on DWI and MG according to lesion size. While MG missed malignant lesions of all sizes, DWI + TIRM only missed benign lesions

Discussion

Women with dense breasts comprise roughly half of the U.S. female population that undergo routine breast cancer screening. Breast cancer mortality has decreased by 39%

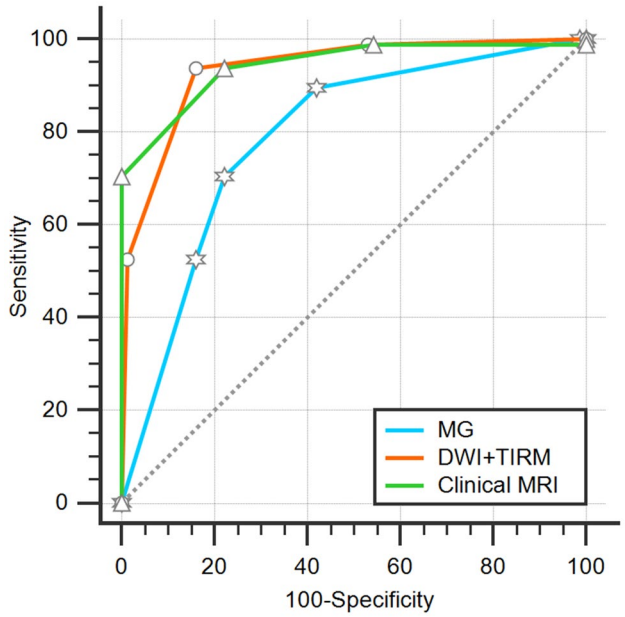

Fig. 7 ROC curves for discrimination of benign and malignant tumors of MG, DWI + TIRM, and Clinical MRI. The AUC of MG was significantly inferior to DWI + TIRM and clinical MRI ($p < 0.001$). No significances regarding AUC were found between DWI + TIRM and clinical MRI

from 1989 to 2015. [30]. This decrease is due, in part, to the detection of small tumors at their early stages by routine breast cancer screening. Unfortunately, there is no sensitive and practical imaging technique without safety concerns to screen women with dense breasts. MG has low sensitivity in dense breasts and leads to missed lesions [7]. Ultrasound has a high rate of false-positive findings that can lead to unnecessary biopsies [31]. Contrast-enhanced MRI is included in the standard protocol for screening women with high risk of breast cancer. Recent studies have demonstrated that gadolinium-based contrast agents (Gd) can accumulate in the brain and other organs [15–18]. The accumulation of interstitial waste products including beta-amyloid in the brain has been suggested to be the cause and progression of numerous neurodegenerative diseases [32, 33]. Compared to iron, gadolinium does not naturally exist in the brain and is a much more toxic element. However, there is currently no documented association between the accumulation of gadolinium and organ toxicity. Carefully designed animal and human studies are needed to fully answer this extremely important question, which is beyond the scope of this study. In brief, there is an urgent need for an alternative imaging technique for the approximately 50% of women with dense breasts. In this study, we have demonstrated that lesion visibility, detection sensitivity, and accuracy of DWI + TIRM were significantly superior to MG in women with dense breasts, and no significant difference was noted when compared with clinical MRI. These results indicate that DWI + TIRM has the potential to simultaneously address detection sensitivity and safety concerns in screening women with dense breasts.

The most important role of screening is to detect all tumors, particularly those that are malignant. In this study, 10 malignant lesions were missed by MG while no malignant lesions were missed by DWI + TIRM. In regard to benign lesions, MG missed 47 while DWI missed 6. The reason for better performance of DWI + TIRM compared to MG likely lies in the nature of DWI and TIRM. As functional imaging, DWI is sensitive to microcellular environmental changes induced by tumors. Moreover, DWI portrays most tumors as a bright signal, thus behaving like a natural contrast agent. In addition to the functional information provided by DWI, TIRM adds anatomic information, further improving tumor detection sensitivity. By comparison, MG does not offer functional information.

Spatial resolution is an important technical factor in detection sensitivity because high spatial resolution is required to detect small tumors. In this study, all lesions invisible on DWI + TIRM were less than or equal to 8 mm. This may be attributed to the spatial resolution of DWI used which was $1.8 \times 1.6 \times 4.0$ mm^3. TIRM in this study had a spatial resolution of $1.1 \times 0.8 \times 4.0$ mm^3 which complimented the relatively poor spatial resolution of DWI. The highest spatial resolution applied to breast DWI in the literature is $0.59 \times 0.59 \times 3.0$ mm^3 [34]. Studies have demonstrated that in addition to functional information, high-resolution DWI can also provide morphological details useful to identifying breast cancers, which is beyond the capability of current screening DWI [34–36]. High spatial resolution DWI should be used for screening in the future and is expected to improve detection sensitivity and specificity. Several ultra-high spatial resolution DWI techniques have been developed for the brain which could be translated for breast in the future [37, 38].

The higher lesion detection sensitivity and accuracy of breast cancer using DWI + TIRM compared to MG are consistent with the literature [39–50]. Previous publications

Table 4 ROC curve analysis for discrimination of benign and malignant tumors of MG, DWI + TIRM, and clinical MRI

	AUC	95% CI	Sensitivity	Specificity	Youden index	Cutoff	*p*
Clinical MRI	0.944	0.899–0.973	93.68	77.78	0.7146	3	< 0.001
DWI + TIRM	0.935	0.888–0.967	93.68	83.95	0.7763	3	< 0.001
MG	0.783	0.714–0.841	46.32	98.77	0.4508	3	< 0.001

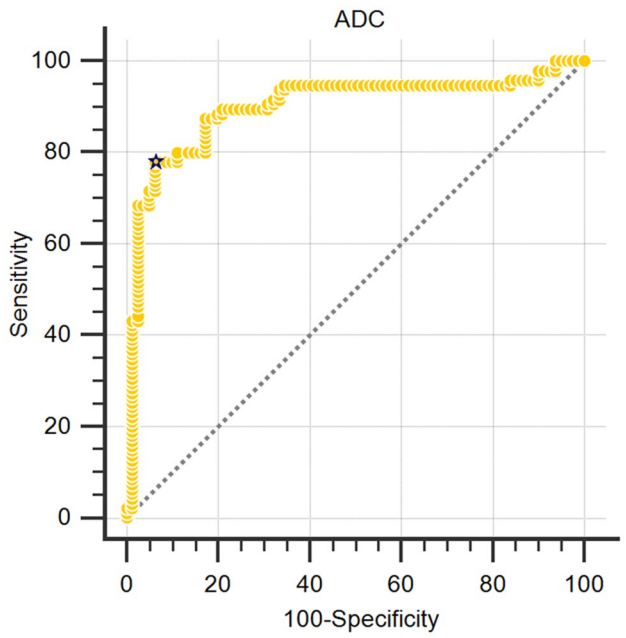

Fig. 8 ROC curve for discrimination of benign and malignant tumors by ADC values

have demonstrated that DWI and T2-weighted images provided a lesion diagnostic accuracy and sensitivity similar to contrast-enhanced MRI [39, 40]. Concordant with this study, Yabuuchi et al. showed that DWI and short time inversion recovery (STIR) images had higher lesion diagnostic accuracy and sensitivity in detecting non-palpable breast cancer compared to MG [39, 46]. This is the first DWI study specifically designed to address the safety concerns with using MRI to screen women with high risk of breast cancer and the sensitivity concerns of using MG to screen women with dense breasts. Poor spatial resolution of DWI typically used in previous studies made DWI a secondary tool rather than a primary tool for breast cancer detection.

Besides safety concerns, the most important practical issue for using MRI as a primary screening tool is its cost and examination duration [49]. In this study, our DWI acquisition time was only 2 min 56 s and the total acquisition time with TIRM is about 4 min, which is about five times less than standard breast MRI protocols. The lack of contrast agent administration further reduces the cost. The safety, sensitivity, and low cost of our proposed MRI technique make it possible to be adopted as a cost-effective routine screening tool in the future, particularly for patients with dense breasts.

This study has several limitations. The most important limitation is that the study population was retrieved from patient lists in the hospital, as opposed to populations that would routinely undergo breast cancer screening. Although our patient population is suitable for the purpose of this feasibility study, prospective screening studies with a large, routine screening-appropriate population are needed to arrive at a definite conclusion. Secondly, given the inclusion criteria for this study it is impossible to be completely blinded. Patients in the study dataset necessarily met the inclusion criteria of having undergone MG, MRI, and pathology. This inclusion criteria thus suggested that the patients had a high risk of having a lesion. Given this limitation, it is possible that readers were more likely to scrutinize the examinations. Additionally, women in China have a relatively earlier age of onset of breast cancer than in the US [50, 51]. With respect to this young age of onset, women in China are more likely to undergo MRI exams for breast cancer screening as opposed to their relatively more elderly counterparts. Another limitation is the lack of comparison between DWI and Digital Breast Tomosynthesis imaging (DBT) or other X-ray-based techniques that have been proposed to overcome the sensitivity problem for women with dense breasts [52–57]. Studies demonstrated that DBT has higher sensitivity than MG, but lower sensitivity than MRI for women with dense breasts [53, 57].

Conclusion

The recent discovery of deposition of MRI contrast agents in the body of even healthy subjects raises concerns regarding the safety of current standard MRI protocols for breast cancer screening. This study demonstrates that lesion visibility, accuracy, and sensitivity of DWI + TIRM were significantly superior to MG in women with dense breasts and comparable with clinical MRI. These findings, along with the short acquisition time and cost effectiveness, suggest that the combination of DWI + TIRM has the potential to simultaneously address sensitivity, safety, and cost in breast cancer screening for women with dense breasts.

Author contributions XZ, JW, SW, and JH conceived and designed the study. SW, MX, YY, and YB enrolled the patients eligible for the study. XZ, MX, YY, and YB performed the analysis and interpretation of data. XZ, JW, YB, and SW drafted the manuscript. JH, BJ, AZ, and KS revised the manuscript critically. All authors read and approved the final manuscript.

Funding This work was supported by the Chinese medicine research foundation project of Zhejiang Province (Grant Number 2018ZA037); Zhejiang provincial medicine and health discipline platform project (Grant Number 2018RC058); Zhejiang provincial health department platform backbone project (Grant Number 2016147237).

Data availability All datasets analyzed during the present study are available from the corresponding author on reasonable request.

Compliance with ethical standards

Conflict of interest This work is supported in part by research grants from Chinese medicine research foundation project of Zhejiang Province, Zhejiang provincial medicine and health discipline platform project, and Zhejiang provincial health department platform backbone project.

Ethical approval The institutional review board of the 1st Affiliated Hospital of Zhejiang Chinese Medical University approved the protocol (2018-KL-017-01).

References

1. Sprague BL, Gangnon RE, Burt V, Trentham-Dietz A, Hampton JM, Wellman RD, Kerlikowske K, Miglioretti DL (2014) Prevalence of mammographically dense breasts in the United States. J Natl Cancer Inst. https://doi.org/10.1093/jnci/dju255
2. Liu J, Liu PF, Li JN, Qing C, Ji Y, Hao XS, Zhang XN (2014) Analysis of mammographic breast density in a group of screening chinese women and breast cancer patients. Asian Pac J Cancer Prev: APJCP 15(15):6411–6414
3. Nelson HD, Zakher B, Cantor A, Fu R, Griffin J, O'Meara ES, Buist DS, Kerlikowske K, van Ravesteyn NT, Trentham-Dietz A et al (2012) Risk factors for breast cancer for women aged 40 to 49 years: a systematic review and meta-analysis. Ann Intern Med 156(9):635–648
4. McCormack VA, dos Santos Silva I (2006) Breast density and parenchymal patterns as markers of breast cancer risk: a meta-analysis. Cancer Epidemiol Biomarkers & Prev 15(6):1159–1169
5. Kerlikowske K, Ichikawa L, Miglioretti DL, Buist DS, Vacek PM, Smith-Bindman R, Yankaskas B, Carney PA, Ballard-Barbash R (2007) Longitudinal measurement of clinical mammographic breast density to improve estimation of breast cancer risk. J Natl Cancer Inst 99(5):386–395
6. Welch HG, Prorok PC, O'Malley AJ, Kramer BS (2016) Breast-cancer tumor size, overdiagnosis, and mammography screening effectiveness. N Engl J Med 375(15):1438–1447
7. Mandelson MT, Oestreicher N, Porter PL, White D, Finder CA, Taplin SH, White E (2000) Breast density as a predictor of mammographic detection: comparison of interval- and screen-detected cancers. J Natl Cancer Inst 92(13):1081–1087
8. Kolb TM, Lichy J, Newhouse JH (2002) Comparison of the performance of screening mammography, physical examination, and breast US and evaluation of factors that influence them: an analysis of 27,825 patient evaluations. Radiology 225(1):165–175
9. Melnikow J, Fenton JJ, Whitlock EP, Miglioretti DL, Weyrich MS, Thompson JH, Shah K (2016) Supplemental screening for breast cancer in women with dense breasts: a systematic review for the U.S. Preventive Services Task Force. Ann Intern Med 164(4):268–278
10. Scheel JR, Lee JM, Sprague BL, Lee CI, Lehman CD (2015) Screening ultrasound as an adjunct to mammography in women with mammographically dense breasts. Am J Obstet Gynecol 212(1):9–17
11. Geisel J, Raghu M, Hooley R (2018) The role of ultrasound in breast cancer screening: the case for and against ultrasound. Semin Ultrasound CT MR 39(1):25–34
12. Peairs KS, Choi Y, Stewart RW, Sateia HF (2017) Screening for breast cancer. Semin Oncol 44(1):60–72
13. Saslow D, Boetes C, Burke W, Harms S, Leach MO, Lehman CD, Morris E, Pisano E, Schnall M, Sener S et al (2007) American Cancer Society guidelines for breast screening with MRI as an adjunct to mammography. CA: Cancer J Clin 57(2):75–89
14. Warner E, Messersmith H, Causer P, Eisen A, Shumak R, Plewes D (2008) Systematic review: using magnetic resonance imaging to screen women at high risk for breast cancer. Ann Intern Med 148(9):671–679
15. Beckett KR, Moriarity AK, Langer JM (2015) Safe use of contrast media: what the radiologist needs to know. Radiographics 35(6):1738–1750
16. Kanda T, Fukusato T, Matsuda M, Toyoda K, Oba H, Kotoku J, Haruyama T, Kitajima K, Furui S (2015) Gadolinium-based contrast agent accumulates in the brain even in subjects without severe renal dysfunction: evaluation of autopsy brain specimens with inductively coupled plasma mass spectroscopy. Radiology 276(1):228–232
17. Gadolinium-containing contrast agents—European Medicines Agency (2018) European Medicines Agency. https://www.ema.europa.eu/en/medicines/human/referrals/gadolinium-containing-contrast-agents. Accessed 5 Feb 2019
18. Ramalho M et al (2017) Gadolinium retention and toxicity—an update. Adv Chronic Kidney Dis 24(3):138–146
19. Malayeri AA, El Khouli RH, Zaheer A, Jacobs MA, Corona-Villalobos CP, Kamel IR, Macura KJ (2011) Principles and applications of diffusion-weighted imaging in cancer detection, staging, and treatment follow-up. Radiographics 31(6):1773–1791
20. Koh DM, Collins DJ (2007) Diffusion-weighted MRI in the body: applications and challenges in oncology. AJR Am J Roentgenol 188(6):1622–1635
21. Palle L, Reddy B (2009) Role of diffusion MRI in characterizing benign and malignant breast lesions. Indian J Radiol Imaging 19(4):287–290
22. Partridge SC, McDonald ES (2013) Diffusion weighted magnetic resonance imaging of the breast: protocol optimization, interpretation, and clinical applications. Magn Reson Imaging Clin N Am 21(3):601–624
23. Guo Y, Cai YQ, Cai ZL, Gao YG, An NY, Ma L, Mahankali S, Gao JH (2002) Differentiation of clinically benign and malignant breast lesions using diffusion-weighted imaging. J Magn Reson Imaging: JMRI 16(2):172–178
24. Kazama T, Kuroki Y, Kikuchi M, Sato Y, Nagashima T, Miyazawa Y, Sakakibara M, Kaneoya K, Makimoto Y, Hashimoto H et al (2012) Diffusion-weighted MRI as an adjunct to mammography in women under 50 years of age: an initial study. J Magn Reson Imaging: JMRI 36(1):139–144
25. McDonald ES, Hammersley JA, Chou SH, Rahbar H, Scheel JR, Lee CI, Liu CL, Lehman CD, Partridge SC (2016) Performance of DWI as a rapid unenhanced technique for detecting mammographically occult breast cancer in elevated-risk women with dense breasts. AJR Am J Roentgenol 207(1):205–216
26. Hauer MP, Uhl M, Allmann K-H, Laubenberger J, Zimmerhackl LB, Langer M (1998) Comparison of turbo inversion recovery magnitude (TIRM) with T2-weighted turbo spin-echo and T1-weighted spin-echo MR imaging in the early diagnosis of acute osteomyelitis in children. Pediatr Radiol 28(11):846–850
27. Sadick M, Sadick H, Hormann K, Duber C, Diehl SJ (2005) Diagnostic evaluation of magnetic resonance imaging with turbo inversion recovery sequence in head and neck tumors. Eur Arch Otorhinolaryngol 262(8):634–639
28. D'Orsi CJ (2013) ACR BI-RADS Atlas: Breast Imaging Reporting and Data System: American College of Radiology
29. DeLong ER, DeLong DM, Clarke-Pearson DL (1988) Comparing the areas under two or more correlated receiver operating characteristic curves: a nonparametric approach. Biometrics 44(3):837–845
30. DeSantis CE, Ma J, Goding Sauer A, Newman LA, Jemal A (2017) Breast cancer statistics, 2017, racial disparity in mortality by state. CA Cancer J Clin 67:439–448

31. Gartlehner G, Thaler K, Chapman A, Kaminski-Hartenthaler A, Berzaczy D, Van Noord MG, Helbich TH (2013) Mammography in combination with breast ultrasonography versus mammography for breast cancer screening in women at average risk. Cochrane Database Syst Rev 4:Cd009632
32. Iliff JJ et al (2012) A paravascular pathway facilitates CSF flow through the brain parenchyma and the clearance of interstitial solutes, including amyloid. Sci Transl Med 4(147):147ra111
33. Tarasoff-Conway JM et al (2015) Clearance systems in the brain—implications for Alzheimer disease. Nat Rev Neurol 11(8):457–470
34. Shin HJ, Park JY, Shin KC, Kim HH, Cha JH, Chae EY, Choi WJ (2016) Characterization of tumor and adjacent peritumoral stroma in patients with breast cancer using high-resolution diffusion-weighted imaging: correlation with pathologic biomarkers. Eur J Radiol 85(5):1004–1011
35. Bogner W, Pinker-Domenig K, Bickel H, Chmelik M, Weber M, Helbich TH, Trattnig S, Gruber S (2012) Readout-segmented echo-planar imaging improves the diagnostic performance of diffusion-weighted MR breast examinations at 3.0 T. Radiology 263(1):64–76
36. Barentsz MW, Taviani V, Chang JM, Ikeda DM, Miyake KK, Banerjee S, van den Bosch MA, Hargreaves BA, Daniel BL (2015) Assessment of tumor morphology on diffusion-weighted (DWI) breast MRI: diagnostic value of reduced field of view DWI. J Magn Reson Imaging: JMRI 42(6):1656–1665
37. van de Bank BL et al (2012) Ultra high spatial and temporal resolution breast imaging at 7T. NMR Biomed 26(4):367–375
38. Springer E et al (2016) Comparison of routine brain imaging at 3T and 7T. Invest Radiol 51(8):469–482
39. Baltzer PA, Benndorf M, Dietzel M, Gajda M, Camara O, Kaiser WA (2010) Sensitivity and specificity of unenhanced MR mammography (DWI combined with T2-weighted TSE imaging, ueMRM) for the differentiation of mass lesions. Eur Radiol 20(5):1101–1110
40. Bickelhaupt S, Tesdorff J, Laun FB, Kuder TA, Lederer W, Teiner S, Maier-Hein K, Daniel H, Stieber A, Delorme S et al (2017) Independent value of image fusion in unenhanced breast MRI using diffusion-weighted and morphological T2-weighted images for lesion characterization in patients with recently detected BI-RADS 4/5 x-ray mammography findings. Eur Radiol 27(2):562–569
41. Lehman CD (2006) Role of MRI in screening women at high risk for breast cancer. J Magn Reson Imaging 24(5):964–970
42. Lehman CD, Blume JD, Weatherall P et al (2005) Screening women at high risk for breast cancer with mammography and magnetic resonance imaging. Cancer 103:1898–1905
43. Podo F, Sardanelli F, Canese R et al (2002) The Italian multi-centre project on evaluation of MRI and other imaging modalities in early detection of breast cancer in subjects at high genetic risk. J Exp Clin Cancer Res 21:115–124
44. Tilanus-Linthorst MM, Obdeijn IM, Bartels KC, de Koning HJ, Oudkerk M (2000) First experiences in screening women at high risk for breast cancer with MR imaging. Breast Cancer Res Treat 63:53–60
45. Morris EA, Liberman L, Ballon DJ et al (2003) MRI of occult breast carcinoma in a high-risk population. AJR Am J Roentgenol 181:619–626
46. Yabuuchi H, Matsuo Y, Sunami S, Kamitani T, Kawanami S, Setoguchi T, Sakai S, Hatakenaka M, Kubo M, Tokunaga E et al (2011) Detection of non-palpable breast cancer in asymptomatic women by using unenhanced diffusion-weighted and T2-weighted MR imaging: comparison with mammography and dynamic contrast-enhanced MR imaging. Eur Radiol 21(1):11–17
47. Kuhl CK, Schrading S, Leutner CC et al (2005) Mammography, breast ultrasound, and magnetic resonance imaging for surveillance of women at high familial risk for breast cancer. J Clin Oncol 23:8469–8476
48. Warner E, Plewes DB, Shumak RS, Catzavelos GC, Di Prospero LS, Yaffe MJ, Goel V, Ramsay E, Chart PL, Cole DEC, Taylor GA, Cutrara M, Samuels TH, Murphy JP, Murphy JM, Narod SA (2001) Comparison of breast magnetic resonance imaging, mammography, and ultrasound for surveillance of women at high risk for hereditary breast cancer. J Clin Oncol 19(15):3524–3531
49. Kuhl CK, Schrading S, Strobel K, Schild HH, Hilgers R-D, Bieling HB (2014) Abbreviated breast magnetic resonance imaging (MRI): first postcontrast subtracted images and maximum-intensity projection—a novel approach to breast cancer screening with MRI. J Clin Oncol 32(22):2304–2310
50. Fan L, Strasserweippl K, Li JJ et al (2014) Breast cancer in China. Lancet Oncol 15(7):e279–e289
51. Li H, Zheng R, Zhang S et al (2018) Incidence and mortality of female breast cancer in China, 2014. Chin J Cancer 40(3):166–171
52. Kriege M, Brekelmans CT, Boetes C et al (2004) Efficacy of MRI and mammography for breast-cancer screening in women with a familial or genetic predisposition. N Engl J Med 351:427–437
53. Phi XA, Tagliafico A, Houssami N et al (2018) Digital breast tomosynthesis for breast cancer screening and diagnosis in women with dense breasts—a systematic review and meta-analysis. BMC Cancer 18(1):380
54. Skaane P, Bandos AI, Gullien R et al (2013) Comparison of digital mammography alone and digital mammography plus tomosynthesis in a population-based screening program. Radiology 267(1):47–56
55. Gur D, Abrams GS, Chough DM et al (2009) Digital breast tomosynthesis: observer performance study. AJR Am J Roentgenol 193(2):586–591
56. Roganovic D, Djilas D, Vujnovic S et al (2015) Breast MRI, digital mammography and breast tomosynthesis: comparison of three methods for early detection of breast cancer. Bosn J Basic Med Sci 15(4):64–68. https://doi.org/10.17305/bjbms.2015.616
57. Förnvik D, Kataoka M, Iima M, Ohashi A, Kanao S, Toi M, Togashi K (2018) The role of breast tomosynthesis in a predominantly dense breast population at a tertiary breast centre: breast density assessment and diagnostic performance in comparison with MRI. Eur Radiol 28(8):3194–3203. https://doi.org/10.1007/s00330-017-5297-7

Affiliations

Yangyang Bu[1,2] · Jun Xia[3] · Bobby Joseph[4] · Xianjing Zhao[1,2] · Maosheng Xu[1,2] · Yingxing Yu[1,2] · Shouliang Qi[5] · Kamran A. Shah[4] · Shiwei Wang[1,2] · Jiani Hu[4]

Yangyang Bu
56386012@qq.com

Jun Xia
xiajun@email.szu.edu.cn

Bobby Joseph
bjoseph2@dmc.org

Xianjing Zhao
xianjingzhao@qq.com

Maosheng Xu
xums166@zcmu.edu.cn

Yingxing Yu
yyx581117@163.com

Shouliang Qi
qisl@bmie.neu.edu.cn

Kamran A. Shah
kshah@wayne.edu

1 The First Clinical Medical College, Zhejiang Chinese Medical University, Hangzhou 310053, China

2 Department of Radiology, The First Affiliated Hospital of Zhejiang Chinese Medical University, 54 Youdian Road, Hangzhou 310006, China

3 Department of Radiology, The First Affiliated Hospital of Shenzhen University, Health Science Center, Shenzhen Second People's Hospital, Shenzhen 518037, China

4 Department of Radiology, Wayne State University, Detroit, MI 48201, USA

5 Sino-Dutch Biomedical and Information Engineering School of Northeastern University, Shenyang, China